Integrated atomistic chemical imaging and reactive force field molecular dynamic simulations on silicon oxidation

Santoshrupa Dumpala,[1] Scott R. Broderick,[1] Umedjon Khalilov,[2] Erik C. Neyts,[2] Adri C. T. van Duin,[3] J Provine,[4] Roger T. Howe,[4] and Krishna Rajan[1,a)]
[1]*Department of Materials Science and Engineering and Institute for Combinatorial Discovery, Iowa State University, 2220 Hoover Hall, Ames, Iowa 50011, USA*
[2]*Department of Chemistry, PLASMANT Research Group, University of Antwerp, Universiteitsplein 1, B-2610 Wilrijk-Antwerp, Belgium*
[3]*Department of Mechanical and Nuclear Engineering, Penn State University, University Park, Pennsylvania 16801, USA*
[4]*Department of Electrical Engineering, Stanford University, 420 Via Palou Mall, Stanford, California 94305, USA*

(Received 6 October 2014; accepted 20 December 2014; published online 5 January 2015)

In this paper, we quantitatively investigate with atom probe tomography, the effect of temperature on the interfacial transition layer suboxide species due to the thermal oxidation of silicon. The chemistry at the interface was measured with atomic scale resolution, and the changes in chemistry and intermixing at the interface were identified on a nanometer scale. We find an increase of suboxide (SiOx) concentration relative to SiO_2 and increased oxygen ingress with elevated temperatures. Our experimental findings are in agreement with reactive force field molecular dynamics simulations. This work demonstrates the direct comparison between atom probe derived chemical profiles and atomistic-scale simulations for transitional interfacial layer of suboxides as a function of temperature. © *2015 AIP Publishing LLC*. [http://dx.doi.org/10.1063/1.4905442]

Thin silicon dioxide films play an important role in microelectronic applications such as metal-oxide-semiconductor field effect transistors (MOSFETs), solar cells, and optical fibers.[1,2] For these applications, understanding the initial oxidation mechanism and characterizing the resulting suboxides is critical due to the influence of bond configuration and layer thickness on various properties of the material.[3] The alteration of bond-lengths of these suboxides modifies the phonon density of states, the electrical conductivity, and the dielectric relaxation.[4] In addition, Gibbs free energy calculations have shown that tetrahedral oxides are stable while suboxides are unstable, thereby affecting structural properties.[5] Theoretical work has demonstrated that the suboxide species at the interface impact the electronic properties (band structures) and leakage currents.[6] Similarly, other theoretical models have shown variation of substoichiometry with temperature and the resulting optical phonon frequency shifts.[7,8]

A consistent model was previously established for describing the translational layer between the silicon and oxide layers during the film growth.[9,10] Recently, a reactive molecular dynamic (MD) simulation studied the temperature dependence of hyperthermal oxidation of silicon and the corresponding atomic scale growth mechanisms.[11] However, there are no corresponding experimental reports at the same length scale due to lateral resolution and mass sensitivity requirements. The objective of the present work is to study the effect of processing conditions on the interfacial properties using in depth atomic scale characterization and, namely, atom probe tomography (APT).

To date, the experimental characterization of this interfacial layer has been studied using photoelectron spectroscopy,[3,12–16] Medium Energy Ion Scattering Spectroscopy (MEIS) and Secondary Ion Mass Spectroscopy (SIMS),[9,10] Rutherford Backscattering Spectroscopy (RBS),[17] Augur Electron Spectroscopy (AES),[18] and Fourier Transform Infrared Spectroscopy (FTIR).[8] However, few of these studies could detect the different suboxides and their distribution variation with temperature and oxide thickness. Table comparing all these different techniques used for detection of suboxides is provided in the supplementary material. APT offers superior depth and spatial resolution along with high chemical sensitivity and atomic scale quantitative depth profile information. While time-of-flight (TOF)-SIMS offers good chemical sensitivity compared to MEIS and higher depth resolution than XPS, the spatial imaging scale of 100 nm is still not sufficiently sensitive for quantitative analysis of advanced microelectronic devices, possible contamination, and sputter induced artifacts.[19–21]

APT combines atomic imaging, field ion microscopy (FIM), and a TOF mass spectrometer to provide direct space three-dimensional, atomic-scale resolution images of materials with the chemical identities of all the detected atoms.[22] Given the depth resolution of one inter-planar atomic layer, APT provides the highest spatial resolution (0.2 nm achievable) and analytical sensitivity (10 atomic parts per million), which we require for characterizing suboxide interfaces.[23]

The implementation of pulsed laser to atom probe has broadened the application of atom probe to study lower conducting materials and insulators including metal oxides.[23–25] There have been multiple studies on the role of preferential evaporation, evolving tip shape, trajectory aberrations, and the interaction of laser with the material on the

a)Email: krajan@iastate.edu. Telephone: 515-294-2670. Fax: 515-294-5444.

reconstruction.[26–34] We follow a different approach here by studying the role of relative oxidation. As the APT experiments are performed under the same condition, the qualitative role of temperature on the oxidation mechanism is studied. The relative changes in oxidation, and particularly suboxides, due to temperature are then compared with simulations.

By utilizing the spatial and chemical resolution of APT, the chemistry at the interface is measured with atomic scale resolution, and changes in chemistry and intermixing over a few nanometer wide range at the interface is identified. This work demonstrates the first direct comparison between atom probe derived chemical profiles with atomistic-scale simulations to study the oxidation mechanism of silicon. From a methodology perspective, the qualitative agreement between experiment and simulation lays the foundation for using this approach to interpret fundamental mechanisms of materials behavior. In the present study, we investigate the relative changes of interfacial structural and compositional analysis as a function of temperature in silicon oxidation using APT and qualitatively compare with simulations.

The Si needles were oxidized using thermal deposition conditions at a pressure ranging from 1–4 Torr at two different temperatures of 383 K and 548 K. The atom probe measurements were achieved using a laser assisted Local Electrode Atom Probe (LEAP 3000 x-Si). The field evaporation from the atomic layer deposition coated silicon tips was performed using 532 nm–10 ps laser pulses with pulse energy of approximately 0.9–1.0 nJ and a repetition rate of 150 kHz.

The atomic Si oxidation was investigated by reactive MD simulations, employing the Reactive Force Field (ReaxFF).[34] ReaxFF accurately describes bond breaking and formation as well as the expansion of the Si crystal during the oxide formation process, in good agreement with both experimental and density functional theory (DFT) results.[11,35–37] In this work, we use the force field parameters developed by Buehler *et al.*[38] The details of the force field parameters used are provided in the supplementary material.[39] Si(100)[11] reconstructed surface is chosen as the initial structure, with dimensions 21.7 Å × 21.7 Å × 27.1 Å. The structure is subsequently equilibrated at 300 K and 700 K using the Berendsen heat bath (NVT dynamics)[40] for 20 ps with a damping constant of 0.1 ps, and consequently relaxed in the microcanonical ensemble (NVE dynamics) for 10 ps.

The atom probe reconstructions of 3D images were generated focusing on the silicon substrate and oxygen interface at both temperatures. The tips having comparable geometry, and the same laser energy were applied, so any effects preferential evaporation or laser effect on relative measurements could be negligible. Figs. 1(a) and 1(b) show the atom probe reconstructed 3D images of the interfacial regions at 383 K and 548 K, respectively. Each sphere in these images is representative of each atom, with respective color code presented. The diffusion of oxygen into silicon is clearly seen at both temperatures. Also, it is observed that the diffusion of oxygen into silicon is greater at higher temperature (548 K) than at lower temperature (383 K) as shown in Fig. 1 with dashed lines representing the approximate width (nm) of inter-diffusion.

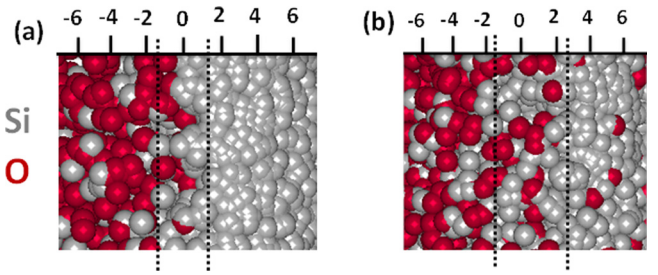

FIG. 1. APT reconstructed 3D images of the silicon and oxygen interface at (a) 383 K and (b) 548 K, with each atom represented in sphere form with the respective color code presented and dashed lines representing interfacial width in nm.

Further thorough analysis of the interfaces can be done by plotting proximity histograms.[41] A proximity histogram is a weighted superposition of concentration profiles plotted across an iso-concentration surface which is chosen as a reference surface. The proximity histograms are plotted across the silicon and silicon oxide interface by choosing an iso-concentration surface of silicon and are shown in Figs. 2(a) and 2(b) for both temperatures. From the figure, a region of inter-diffusion (i.e., interface (region II)) and two distinct regions consisting of bulk silicon (region I) and an oxide phase (region III) can be clearly seen at both temperatures. The interfacial width marked with dashed lines is in close approximation with Fig. 1.

The formation of a thicker interface region at high temperature was also observed in the reactive molecular dynamic simulation work, which is attributed to the increased diffusivity of oxygen, allowing the deeper penetration of oxygen at higher temperatures which in turn slows down the conversion of the Si suboxide components.[11] Namely, due to the decreasing of interfacial stresses[42] in Region II, the mobility of oxygen atoms in the transition region increases. While the thickness of the transition region (Region II) is somewhat smaller in the simulation results, the ratio between the thicknesses at both investigated temperatures agrees quantitatively with the experimental result, at a ratio of about 1.3. While the temperatures are not in total quantitative agreement, our objective is to compare the qualitative findings, given the difference in time-scale between APT and ReaxFF (milliseconds vs. nanoseconds). Agreement between the experimental and simulation results can be seen, both with respect to the Si and O concentrations, as well as the thicknesses of the interface.

We chose temperatures of 300 K and 700 K in the simulations, which are slightly lower and higher than the experimental temperatures, respectively, in order to magnify the observed effects in the change of the transition region thickness in the simulations. This was done because the simulations are confined to the nanosecond time scale. On such short timescales, small differences, as in temperature, for example, are often difficult to observe and study. It is important to realize, however, that in both simulated cases, the oxygen species are not mobile yet in the interface, in agreement with experimental evidence.[43]

Due to the intrinsic limitation on the time scale that can be reached in molecular dynamics simulations, diffusion in the oxidation process is very difficult to capture in these simulations. Experimentally, the diffusion takes place in the

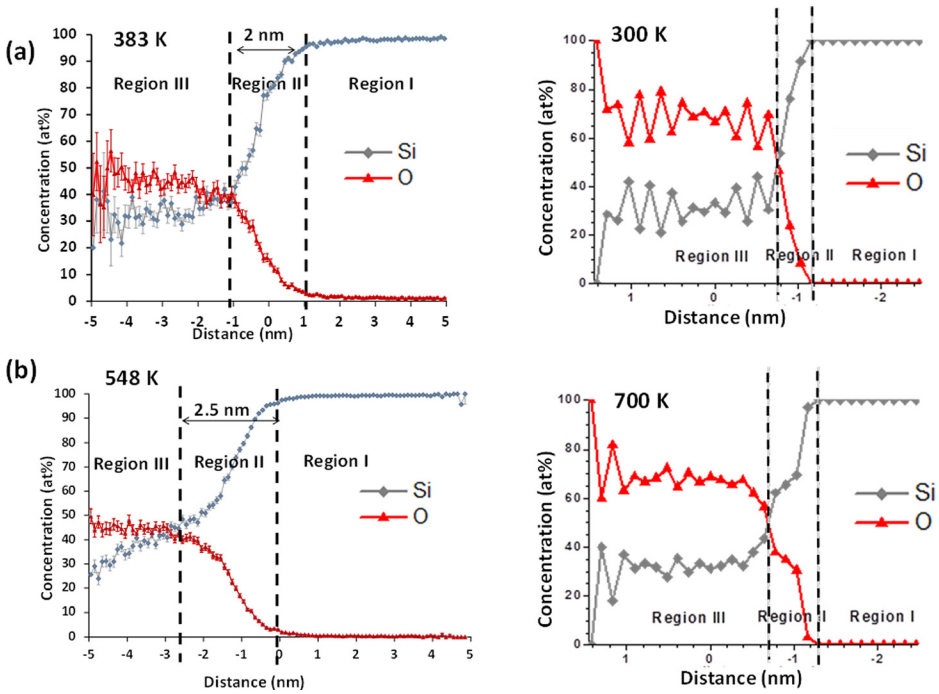

FIG. 2. Diffusion profiles at (a) 383 K and (b) 548 K. Bulk silicon (region I), interface (region II), and the bulk oxide (region III) phases can be clearly seen. The left figures are the APT results, while the right figures are ReaxFF simulation results.

millisecond time scale, whereas the MD is limited to the nanosecond time scale. Therefore, the difference in thickness between simulation and experiment is due to the limitation in simulation time, and the observed agreement is qualitative.

Further analysis of the oxidation mechanism in terms of the various suboxide species that were formed at various stages of the oxidation at different temperature is done in comparison with the simulations. Fig. 3 shows the proxigrams plotted, indicating the concentration of various suboxide species, particularly at the different regions identified in Fig. 2. The various suboxide species detected through APT such as SiO, Si_2O, and SiO_2 correspond to their respective valence states of silicon such as Si^{+}, Si^{2+}, and Si^{4+}. It was observed that the interfacial region marked as region II consists of a greater amount of suboxide species (clearly seen from the bar charts of Figs. 3(c) and 3(d)) which is in agreement with the simulation results. We do see the presence of some of these suboxides even in the silicon oxide region III, which can be related to possible presence of over-coordinated and under-coordinated Si atoms that were assumed to be found in this region as per simulations.[11] Also, it was reported that the observed silica region can be divided into surface and bulk regions.[36] In the present case, we refer to a surface silica region and a bulk silica region.

Further agreement of the effect of temperature on growth mechanisms in comparison with ReaxFF simulation results is clearly shown in Fig. 4. Quantitative details of atomic scale intermixing at Si/O interface can be seen from

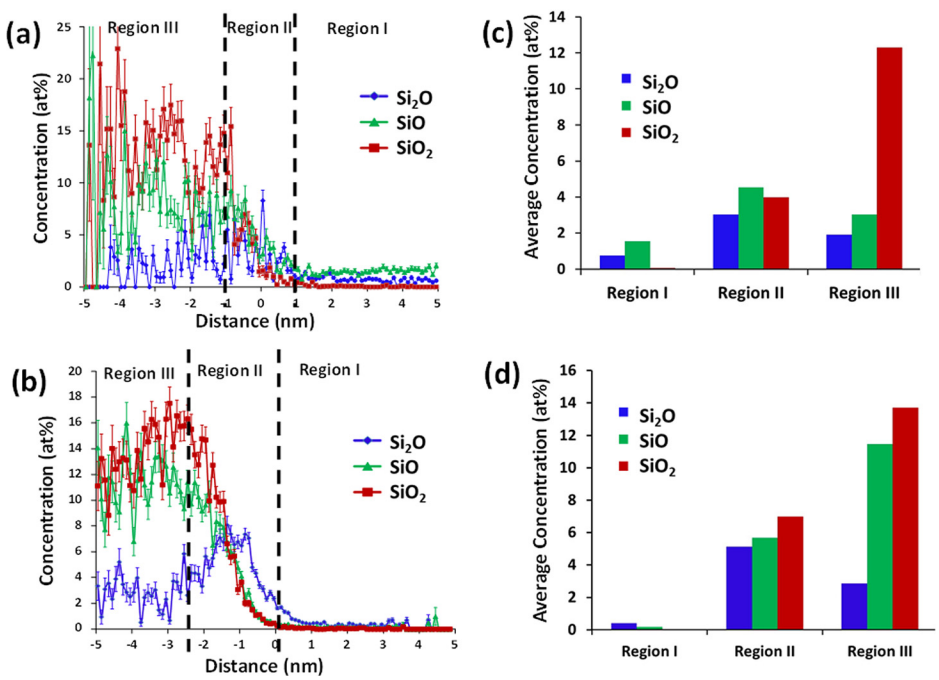

FIG. 3. (a) and (b) showing the diffusion profiles of SiO_2 and SiO_x ($x < 2$) and respective bar charts representing the percentage concentration of the oxides in the three different regions at 383 K and 548 K, respectively.

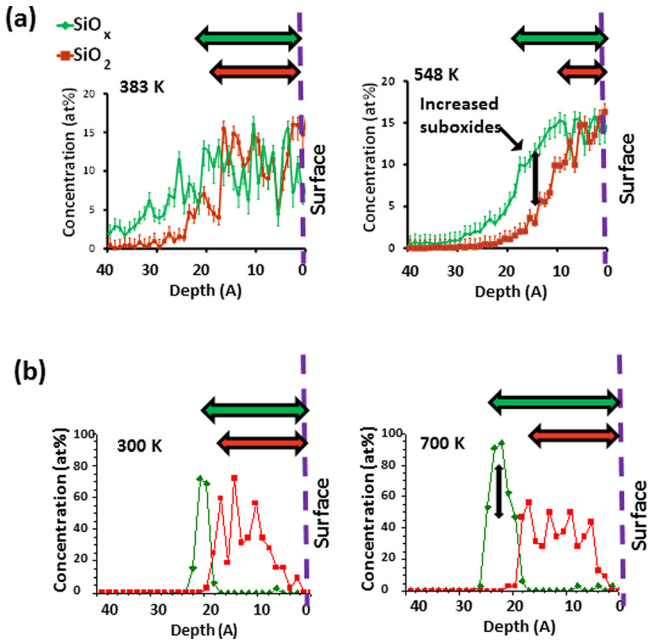

FIG. 4. (a) Atom probe experimental results of concentration profiles (left 383 K and right 548 K) plotted in proxigrams at both temperatures and (b) ReaxFF simulations (left 300 K and right 700 K) showing qualitative agreement with the trend of both oxide chemistries including SiO_2 (red) and SiOx (total sub-oxide species including SiO and Si_2O) (green).

(a) atom probe concentration profiles; and (b) verification that the findings are consistent with simulations. Two profiles are shown: one for an experiment at ~300 K (left) and another at ~500 K.

The trends of SiO_2 and SiOx (representing the total detected sub-oxide species including SiO and Si_2O) that are detected at both temperatures qualitatively agree with the trend observed from simulations. At the lower temperature, the relative concentrations and penetration depths of the two oxides (highlighted by green and red arrows) are qualitatively same from the oxide/gas surface, as shown in Fig. 4(a). At the higher temperature, the relative concentration (highlighted by the black arrow) and penetration depth of sub-oxide are significantly higher than that of SiO_2.

From Fig. 4(b), it is clearly seen that similar oxides and sub-oxides are detected by the simulation studies at both temperatures in agreement with the experimental observations. The increase of suboxide (SiOx) concentration relative to SiO_2 and increased oxygen ingress seen by increased penetration depth of suboxides at increasing temperature qualitatively agrees well with the experimental observations. The experimental results at higher temperature agree with the value being greater than the threshold (>500 K).[11]

For more clarity, the increased concentration of suboxides (highlighted by the black arrow) and the increased penetration depth of suboxides (highlighted by green and red arrows) than SiO_2 at higher temperature in experimental results and simulations are shown in Figs. 4(a) and 4(b), respectively.

This work provides experimental insight into the atomic scale characterization of the transitional layer of suboxides and oxides of oxidized silicon substrate. Various oxide species including different suboxides and intermixing at the interfaces were analyzed as a function of oxidation temperature. From the results, we find that at higher temperature there is an increase of suboxide (SiOx) concentration relative to SiO_2 and increased oxygen ingress compared to lower temperatures. The increase of the oxygen ingress is clearly seen from the concentration profiles with increased interfacial width. Despite the difference in time scales of the experiments and simulations, there is a qualitative agreement between the atomistic-scale ReaxFF simulation results and atom probe results. This work demonstrates the direct comparison between atom probe derived chemical imaging and profiles with atomistic-scale simulations based profiles. From the methodology perspective, the agreement between the experimental characterization and molecular dynamics simulations lays the foundation for using this approach of combining APT with atomic simulations to interpret fundamental interfacial mechanisms of materials behavior.

We acknowledge the support of the Air Force Office of Scientific Research (AFOSR) under Grant No. FA9550-11-1-0158. S.D., S.B., and K.R. acknowledge support under AFOSR Grant No. FA9550-12-1-0456 and NSF Grant Nos. PHY CDI-09-41576 and ARI Program CMMI-09-389018. The work was carried out in part using the Turing HPC infrastructure of the CalcUA core facility of the Universiteit Antwerpen, a division of the Flemish Supercomputer Center VSC, funded by the Hercules Foundation, the Flemish Government (department EWI), and the Universiteit Antwerpen. K.R. also acknowledges support from the Wilkinson Professorship of Interdisciplinary Engineering.

[1]M. A. Green, Nanotechnology **11**(4), 401 (2000).
[2]A. M. Stoneham, J. Non-Cryst. Solids **303**(1), 114 (2002).
[3]T. Hattori and T. Suzuki, Appl. Phys. Lett. **43**(5), 470 (1983).
[4]P. Carrier, L. J. Lewis, and M. W. C. Dharma-Wardana, Phys. Rev. B **64**(19), 195330 (2001).
[5]D. R. Hamann, Phys. Rev. B **61**(15), 9899 (2000).
[6]B. H. Kim, G. Kim, K. Park, M. Shin, Y. C. Chung, and K. R. Lee, J. Appl. Phys. **113**(7), 073705 (2013).
[7]A. R. Chowdhuri, D. U. Jin, J. Rosado, and C. G. Takoudis, Phys. Rev. B **67**(24), 245305 (2003).
[8]H. Ono, T. Ikarashi, K. Ando, and T. Kitano, J. Appl. Phys. **84**(11), 6064 (1998).
[9]E. P. Gusev, H. C. Lu, T. Gustafsson, and E. Garfunkel, Phys. Rev. B **52**(3), 1759 (1995).
[10]T. F. Zeng and H. C. Doumanidis, "A study on growth of ultrathin silicon dioxide films by rapid thermal oxidation," in *Technical Proceedings of the 2003 Nanotechnology Conference and Trade Show* (2003), p. 40.
[11]U. Khalilov, G. Pourtois, A. C. T. van Duin, and E. C. Neyts, J. Phys. Chem. C **116**(15), 8649 (2012).
[12]K. Hirose, H. Nohira, T. Koike, K. Sakano, and T. Hattori, Phys. Rev. B **59**(8), 5617 (1999).
[13]J. H. Oh, H. W. Yeom, Y. Hagimoto, K. Ono, M. Oshima, N. Hirashita, M. Nywa, A. Toriumi, and A. Kakizaki, Phys. Rev. B **63**(20), 205310 (2001).
[14]A. Yoshigoe, K. Moritani, and Y. Teraoka, Appl. Surf. Sci. **216**(1–4), 388 (2003).
[15]Z. H. Lu, M. J. Graham, S. P. Tay, D. T. Jiang, and K. H. Tan, J. Vac. Sci. Technol., B **13**(4), 1626 (1995).
[16]K. Hirose, H. Nohira, K. Azuma, and T. Hattori, Prog. Surf. Sci. **82**(1), 3 (2007).
[17]K. Kimura and K. Nakajima, Appl. Surf. Sci. **216**(1–4), 283 (2003).
[18]S. S. Chao, J. E. Tyler, Y. Takagi, P. G. Pai, G. Lucovsky, S. Y. Lin, C. K. Wong, and M. J. Mantini, J. Vac. Sci. Technol., A **4**(3), 1574 (1986).
[19]D. Giubertoni, A. Bersani, M. Barozzi, S. Pederzoli, E. Iacob, J. A. van den Berg, and M. Werner, Appl. Surf. Sci. **252**(19), 7214 (2006).

[20]E. Martinez, P. Ronsheim, J. P. Barnes, N. Rochat, M. Py, M. Hatzistergos, O. Renault, M. Silly, F. Sirotti, F. Bertin, and N. Gambacorti, Microelectron. Eng. **88**(7), 1349 (2011).
[21]S. Messenger, L. P. Keller, F. J. Stadermann, R. M. Walker, and E. Zinner, Science **300**(5616), 105 (2003).
[22]M. K. Miller, T. F. Kelly, K. Rajan, and S. P. Ringer, Mater. Today **15**, 158 (2012).
[23]T. F. Kelly, D. J. Larson, K. Thompson, R. L. Alvis, J. H. Bunton, J. D. Olson, and B. P. Gorman, *Annual Review of Materials Research* (Annual Reviews, Palo Alto, 2007), Vol. 37, p. 681.
[24]C. Oberdorfer, P. Stender, C. Reinke, and G. Schmitz, Microsc. Microanal. **13**(5), 342 (2007).
[25]B. Gault, F. Vurpillot, A. Vella, M. Gilbert, A. Menand, D. Blavette, and B. Deconihout, Rev. Sci. Instrum. **77**(4), 043705 (2006).
[26]M. Muller, D. W. Saxey, G. D. W. Smith, and B. Gault, Ultramicroscopy **111**(6), 487 (2011).
[27]E. A. Marquis, B. P. Geiser, T. J. Prosa, and D. J. Larson, J. Microsc. **241**(3), 225 (2011).
[28]C. Oberdorfer and G. Schmitz, Microsc. Microanal. **17**(1), 15 (2011).
[29]F. Vurpillot, A. Bostel, and D. Blavette, Appl. Phys. Lett. **76**(21), 3127 (2000).
[30]M. Muller, G. D. W. Smith, B. Gault, and C. R. M. Grovenor, J. Appl. Phys. **111**, 064908 (2012).
[31]A. Devaraj, R. Colby, W. P. Hess, D. E. Perea, and S. Thevuthasan, J. Phys. Chem. Lett. **4**(6), 993 (2013).
[32]Y. M. Chen, T. Ohkubo, and K. Hono, Ultramicroscopy **111**(6), 562 (2011).
[33]J. H. Lee, Y. T. Kim, J. J. Kim, S. Y. Lee, and C. G. Park, Electron. Mater. Lett. **9**(6), 747 (2013).
[34]J. H. Lee, B. H. Lee, Y. T. Kim, J. J. Kim, S. Y. Lee, K. P. Lee, and C. G. Park, Micron **58**, 32 (2014).
[35]A. C. T. van Duin, A. Strachan, S. Stewman, Q. S. Zhang, X. Xu, and W. A. Goddard, J. Phys. Chem. A **107**(19), 3803 (2003).
[36]U. Khalilov, E. C. Neyts, G. Pourtois, and A. C. T. van Duin, J. Phys. Chem. C **115**(50), 24839 (2011).
[37]U. Khalilov, G. Pourtois, A. C. T. van Duin, and E. C. Neyts, Chem. Mater. **24**(11), 2141 (2012).
[38]M. J. Buehler, A. C. T. van Duin, and W. A. Goddard, Phys. Rev. Lett. **96**(9), 095505 (2006).
[39]See supplementary material at http://dx.doi.org/10.1063/1.4905442 for the details of the different experimental techniques used previously for characterizing interfaces and the force field parameters used.
[40]H. J. C. Berendsen, J. P. M. Postma, W. F. Vangunsteren, A. Dinola, and J. R. Haak, J. Chem. Phys. **81**(8), 3684 (1984).
[41]O. C. Hellman, J. A. Vandenbroucke, J. Rusing, D. Isheim, and D. N. Seidman, Microsc. Microanal. **6**(5), 437 (2000).
[42]U. Khalilov, G. Pourtois, A. C. T. van Duin, and E. C. Neyts, J. Phys. Chem. C **116**(41), 21856 (2012).
[43]K. Kajihara, T. Miura, H. Kamioka, A. Aiba, M. Uramoto, Y. Morimoto, M. Hirano, L. Skuja, and H. Hosono, J. Non-Cryst. Solids **354**, 224 (2008).